



Technical Note: Benchmark time-temperature paths provide a shared framework for evaluating and communicating thermochronologic data interpretation

Andrea L. Stevens Goddard¹, Kendra E. Murray², Alyssa A. Abbey³, and Mark Wildman⁴

¹Department of Earth and Atmospheric Sciences, Indiana University, 1001 E 10th St.,
Bloomington, IN 47408, USA

²Department of Geosciences, Idaho State University, 921 South 8th Avenue, Pocatello, ID
83209, USA

³Department of Geological Sciences, California State University, Long Beach, 1250 Bellflower
Boulevard, Long Beach, CA 90840, USA

⁴School of Geographical and Earth Sciences, University of Glasgow, 8NN, University Ave,
Glasgow, UK

Correspondence to: Andrea L. Stevens Goddard (alsg@iu.edu)



1 **Abstract.** We present a set of six time-temperature (tT) histories, called benchmark paths, that
2 can be used as a shared framework for evaluating the sensitivity of a thermochronologic system
3 to the variables inherent in the interpretation of thermochronologic data (e.g., kinetics models,
4 mineral compositions or geometries, etc.) . These benchmark paths span 100 Myr, include
5 monotonic and nonmonotonic histories that represent plausible geologic scenarios, and have a
6 range of cooling rates through different chronometer partial-retention/annealing temperatures.
7 Here, we demonstrate their utility by presenting a method for tuning these paths to 11 different
8 kinetics models for the apatite (U-Th-Sm)/He ($n=5$), apatite fission-track ($n=2$), and zircon (U-
9 Th)/He ($n=4$) systems. These tuned tT paths provide a practical comparison of the kinetics
10 models for each system and the data patterns they predict, thereby offering anyone performing
11 thermal history analysis the ability to consider how their choice of kinetics model may impact
12 their data interpretation. The adoption of benchmark paths for evaluating kinetics models and
13 other variables provides a practical way for the thermochronology community to evaluate and
14 communicate the decision making processes that are inherent in thermochronologic modeling
15 and data interpretation.

16

17 **1. Introduction**

18 We propose adopting a common set of thermal (time-temperature, tT) histories, called
19 benchmark paths, for the apatite (U-Th-Sm)/He, apatite fission-track, and zircon (U-Th)/He
20 systems (hereafter AHe, AFT, and ZHe, respectively). These benchmark paths can be used for
21 a variety of applications because they are designed to highlight the sensitivity of each
22 thermochronometric system to differences in kinetics models, tT history features, mineral
23 compositions/geometries, and other variables critical to the interpretation of thermochronologic
24 data. For example, here we demonstrate the utility of these benchmark paths by using them to



25 visualize and quantify the consequences of choosing different kinetics models to interpret
26 cooling ages.

27

28 **2. Designing the benchmark thermal histories**

29 Figure 1 presents a general representation of our proposed benchmark paths, which are
30 inspired by the paths in Wolf et al. (1998) and designed with the following criteria. Together,
31 these paths:

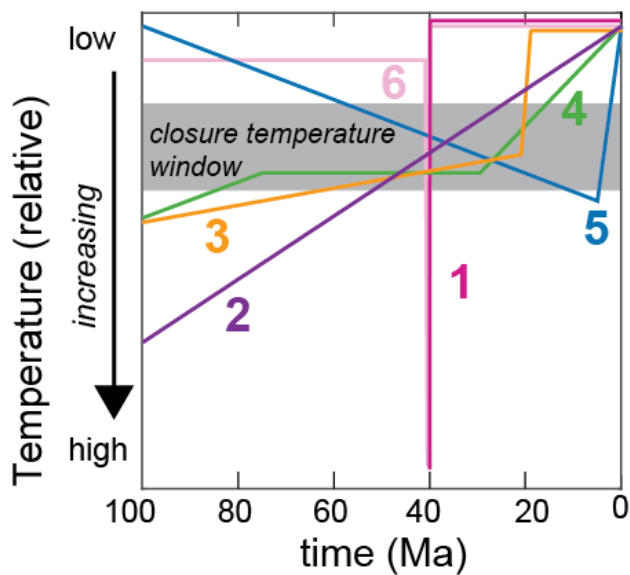
- 32 1. include simulations of both monotonic and non-monotonic thermal histories
- 33 2. explore a range of cooling rates through a chronometer's closure temperature window
- 34 3. represent geologically plausible thermal histories

35 The proposed 100-Myr-long benchmark paths represent distinct but realistic geologic
36 histories that capture simple monotonic cooling (Paths 1, 2) and complete thermal resetting
37 (Path 6), in addition to complex thermal conditions such as sustained residence in the closure
38 temperature window (Paths 3, 4) and reheating that results in partial resetting (Path 5) that tend
39 to produce more complicated data sets.

40 Each of our six proposed benchmark thermal histories are representative of a geologic
41 setting in the following ways. Path 1 simulates rapid cooling, like that associated with post-
42 eruptive cooling of a volcanic rock. Path 2 represents protracted cooling, typical of cratonic
43 erosion. Path 3 represents rapid rock cooling, such as is associated with rift initiation settings.
44 Path 4 shows cooling representative of erosion patterns in emerging topography, like that in an
45 active thrust belt. Path 5 includes heating at rates typical of basin burial followed by cooling
46 associated with basin inversion and exhumation. Path 6 simulates transient localized heating
47 and cooling, similar to what may happen next to a near-surface igneous intrusion. Each of these
48 geologic scenarios has a different duration and rate of cooling through the closure temperature
49 window (Fig. 1).



50 In this contribution, we decided to tune these paths such that they all predict a 40 Ma age for
51 a specific grain composition and/or size because this facilitates an inverse approach. In other
52 words, we visualize the results as the range of tT paths that are all tuned to produce a 40 Ma
53 age, where the tuned differences in the tT paths reflect the consequences of the thermal history
54 model inputs (e.g., kinetics model, etching protocols, grain geometry, mineral chemistry). This
55 mimics the most common thermochronologic workflow, where cooling age(s) are measured and
56 tT modeling is used to find the range of tT histories that fit those data. Designing each
57 benchmark path to produce a single 40 Ma age also means that they inherently demonstrate the
58 nonuniqueness of individual cooling ages (Wolf et al., 1998).



59 *Figure 1: Proposed benchmark paths with relative temperature histories. Paths 1-5 are inspired*
60 *by Wolf et al., (1998) and modified by Murray et al., (2022) demonstrating the non-uniqueness*
61 *of a single cooling age.*



62 3. Tuning benchmark paths to specific kinetics models

63 We demonstrate the utility of our proposed benchmark paths by using them to illustrate
64 the different temperature sensitivities of three low-temperature thermochronometers (AHe, AFT,
65 ZHe), and then, within each system, how kinetics models also require different temperatures to
66 produce the same age. This is useful because although experimentally-derived kinetics models
67 provide the foundation for the interpretation of thermochronologic data, it can be difficult to
68 develop a practical understanding of if or how choosing one kinetics model over another might
69 impact one's thermal history model results. This is critical for both project design and data
70 interpretation.

71 Most publications that introduce new kinetics models use example tT histories that are
72 calibrated to demonstrate the nuances of that specific kinetics model, in addition to the
73 mathematical calibrations that include intrinsic mineral features including chemistry, radiogenic
74 element concentration, and geometries (e.g., Wolf et al., 1996; Carlson et al., 1999; Donelick et
75 al., 1999; Ketcham et al., 1999; Farley, 2000; Reiners et al., 2004; Flowers et al., 2009;
76 Gautheron et al., 2009; Guenther et al., 2013; Willett et al., 2017; Ginster et al., 2019;
77 Guenther, 2021). For example, Flowers et al. (2009) demonstrated the RDAAM AHe kinetics
78 model using the ~300 Myr history of the Esplanade Sandstone and the ~1800 Myr history of
79 basement samples from the Canadian Shield. The α -recoil damage AHe kinetics model was
80 introduced by Gautheron et al. (2009) using the ~300 Myr duration geologic history of the
81 French Massif Central. Willett et al. (2017) uses the predicted ages from a ~550 Myr duration
82 geologic history from the Grand Canyon to present the ADAM AHe kinetics model. These
83 individualized tT histories remain a fundamental contribution because they demonstrated
84 behaviors distinctive to a particular kinetics model and the rocks these models were first applied
85 to. Our benchmark paths complement these contributions by providing a universal reference
86 frame that can be used to compare these kinetics models.



87 All benchmark paths are tuned to produce a 40 Ma age in crystals with the following
88 standard sizes and compositions. For the AHe system, the crystal is assigned a spherical radius
89 (R_s) of 60 μm and an effective uranium concentration ($[eU] = [U] + 0.234*[Th] + 0.0047*[Sm]$) of
90 60 ppm. All benchmark paths are tuned for the AFT system using a $D_{par} = 2.05 \mu\text{m}$ for grains
91 etched in 5.5M HNO_3 for 20 seconds (Sobel & Seward, 2010). All benchmark paths are tuned
92 for the ZHe system using a crystal with $R_s = 60 \mu\text{m}$ and $[eU] = 600$ ppm.

93 To tune a general benchmark path (Fig. 1) to a specific thermochronometer and an
94 associated kinetics model, we held constant the timing of heating and cooling events but
95 modified the maximum temperatures that control the timing and duration of passage through the
96 system's closure temperature window to produce a 40 Ma age (Fig. 2, Table 1). Practically, this
97 requires changing the temperature of one node of the tT path for each kinetics model (Fig. 2,
98 Table 1). Additionally, for each system (AHe, AFT, ZHe), benchmark paths 3 and 4 are
99 assigned an initial temperature at 100 Ma that is necessary for simulating slow cooling or
100 isothermal holding within the chronometer's closure temperature window (Fig. 2, Table 1). Then,
101 we further tuned the benchmark paths for each chronometer to all produce a 40 Ma age using
102 the following specific kinetics models:(1) the AHe system including Wolf et al. (1998), Farley
103 (2000), Flowers et al., (2009), Gautheron et al. (2009), and Willett et al., (2017); (2) the AFT
104 system including Ketcham et al., (1999) and Ketcham et al. (2007); and (3) the ZHe system
105 including Reiners et al., (2004), Guenther et al. (2013), Ginster et al. (2019), and Guenther
106 (2021) implementation of the ZRDAAM without annealing (Fig. 2, Table 1).

107 Within each chronometric system, this exercise provides a sensitivity test of kinetics
108 models. For example, for the AHe, AFT, and ZHe systems, the same temperature conditions
109 predict the same cooling age for rapid cooling associated with igneous processes (Fig. 2, Paths
110 1, 6). This suggests that the choice of a kinetics model in these thermal conditions will not
111 change the interpretation of the data, as has been previously discussed in the papers that



112 originally presented these kinetics models (e.g., Ketcham et al., 1999; Flowers et al., 2009;
113 Guenther et al., 2013).

114 By contrast, paths that feature slow cooling or prolonged residence at and/or reheating
115 to partial retention/annealing temperatures require different temperatures to predict the same
116 cooling age; making the corollary also true: measured cooling age(s) may fit different cooling
117 histories if using different kinetics models (Fig. 2). For example, the thermal histories that
118 produce a Path 4, 40 Ma cooling age for the AHe system require that the crystals are held at
119 temperatures between 75 and 29.5 Ma, but the difference in this holding temperature can vary
120 by nearly 30°C depending on the kinetics model used (Fig. 2). This variability in holding
121 temperatures is much lower, ~ 10°C, for the AHe kinetics models that incorporate the effects of
122 radiation damage and annealing (Flowers et al., 2009; Gautheron et al., 2009; Willett et al.,
123 2017), but could still modify the geologic interpretations of such a data set. Interpretations using
124 kinetics from a legacy AHe kinetics model that does not consider the effects of radiation
125 damage and annealing (e.g., Wolf et al., 1996; Farley, 2000) should be reevaluated. For the
126 AFT system, Path 4 benchmark thermal histories also vary. The legacy kinetics model of
127 Ketcham (1999) requires a retention temperature ~ 10°C higher than the kinetics model of
128 Ketcham et al. (2007). By contrast, Path 4 benchmark thermal histories for ZHe kinetics models
129 from Guenther et al. (2013) and Ginster et al., (2019) differ by only ~ 1°C indicating that the
130 choice of one kinetics model over the other will not modify the interpretation of such a data set.

131 We propose that for any new kinetics model, a new tuned set of benchmark paths is
132 made that can be compared with those tuned to existing kinetics models (Fig. 2). This set of
133 benchmark paths would be tuned by modifying the maximum temperature within the closure
134 temperature window of each mineral system to generate a predicted cooling age of 40 Ma ± 1
135 Ma using a particular kinetics model (Fig. 2, Table 1).

136

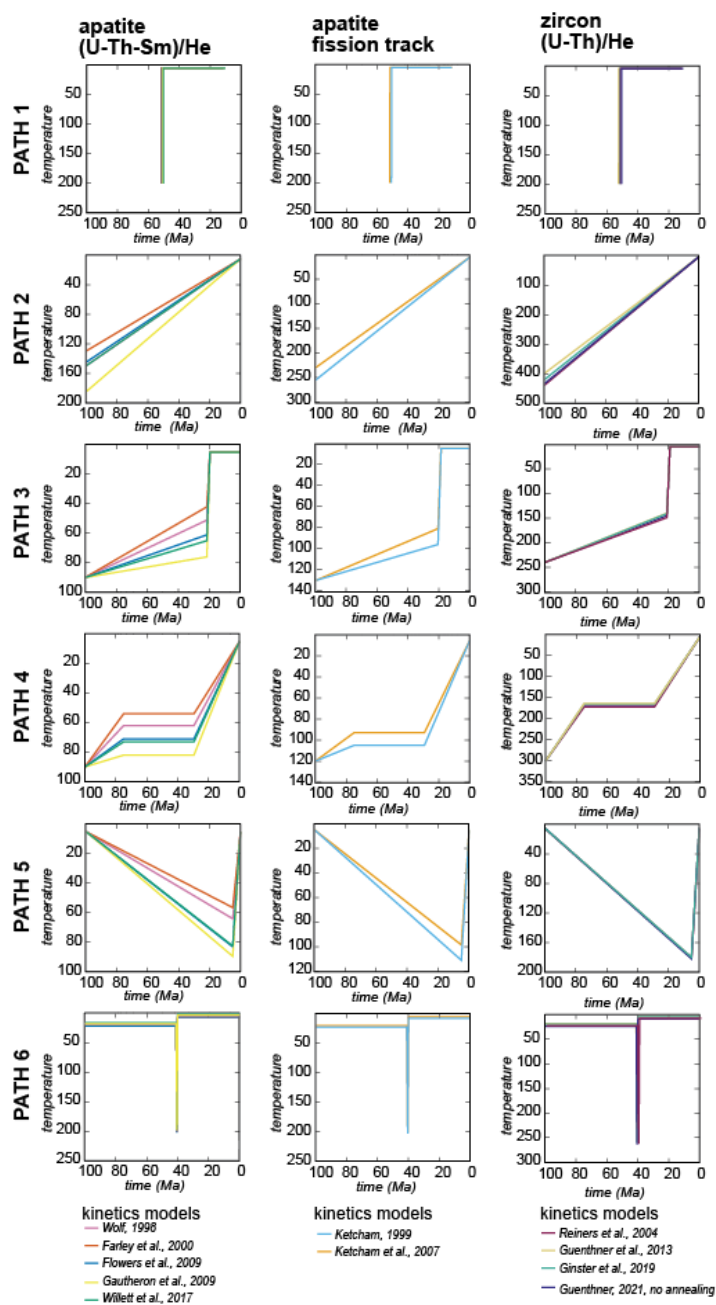
137



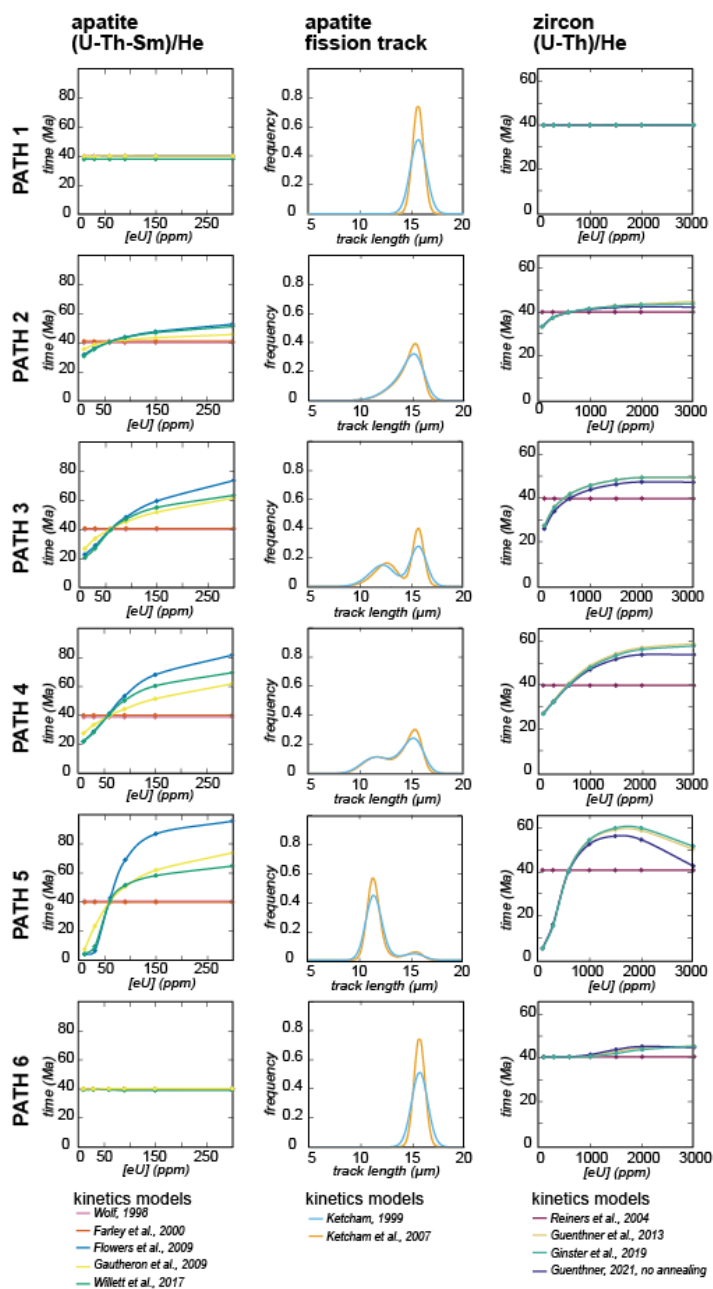
		kinetics model	Path 1			Path 2		Path 3			Path 4			Path 5		Path 6									
		citation	40	39.9	0	100	0	100	21	19	0	100	75	30	0	100	5	0	100	41	40.5	40	0		
		time (Ma)																							
apatite (U-Th)/He	Wolf et al., 1996	Temperature (°C)	200	5	5	150	5	90	51	5	5	90	62	62	5	5	64	5	20	20	200	5	5		
	Farley, 2000	Temperature (°C)	200	5	5	130	5	90	42	5	5	90	54	54	5	5	57	5	20	20	200	5	5		
	Flowers et al., 2009	Temperature (°C)	200	5	5	145	5	90	61	5	5	90	71	71	5	5	83	5	20	20	200	5	5		
	Gautheron et al., 2009	Temperature (°C)	200	5	5	185	5	90	76	5	5	90	82	82	5	5	90	5	20	20	200	5	5		
	Willett et al., 2017	Temperature (°C)	200	5	5	150	5	90	65	5	5	90	73	73	5	5	83	5	20	20	200	5	5		
apatite fission track	Ketcham et al., 2007	Temperature (°C)	200	5	5	230	5	130	81	5	5	120	93	93	5	5	99	5	20	20	200	5	5		
	Ketcham et al., 1999	Temperature (°C)	200	5	5	255	5	130	96	5	5	120	105	105	5	5	111	5	20	20	200	5	5		
zircon (U-Th)/He	Reiners et al., 2004	Temperature (°C)	200	5	5	440	5	240	149	5	5	300	172	172	5	5	180	5	20	20	260	5	5		
	Guenthner et al. 2013	Temperature (°C)	200	5	5	400	5	240	140	5	5	300	164	164	5	5	181	5	20	20	260	5	5		
	Guenthner, 2021	Temperature (°C)	200	5	5	435	5	240	145	5	5	300	168	168	5	5	182	5	20	20	260	5	5		
	Ginster et al., 2019	Temperature (°C)	200	5	5	421	5	240	141	5	5	300	165	165	5	5	180	5	20	20	260	5	5		

change Temperature across
 chronometer
 change Temperature across
 kinetics model

138 Table 1: Benchmark Paths tuned to produce a 40 Ma cooling age for common legacy and
 139 modern kinetics models for the apatite (U-Th)/He, apatite fission track, and zircon (U-Th)/He
 140 systems.



141 Figure 2: Benchmark paths shown in tT space. Benchmark paths are tuned to produce a 40 Ma
 142 cooling age using published legacy and modern kinetics models of the AHe, AFT, and ZHe
 143 systems



144 Figure 3: Expanding the data predicted by benchmark paths to include crystals with a range of
 145 eU (AHe, ZHe) and track length distributions (AFT) shows data trends that can be used to
 146 distinguish among the predictions and interpretations of different kinetics models.



147 **4. Using benchmark paths to visualize the additional effects of compositional variations**
148 **in datasets with more than one analysis**

149 We next use the tuned benchmark paths to predict age-[eU] trends and track-length
150 distributions (Fig. 3). Expanding the predicted results of a benchmark path in these ways
151 simulates the resolving power of a real dataset with multiple analyses and demonstrates how
152 the choice of kinetics model may impact the possible fits to the data.

153 For the AHe and ZHe systems, we used tuned benchmark paths to predict multiple He
154 ages from a range of crystal [eU] compositions and thereby quantify and visualize the potential
155 impact of choosing one kinetics model over another during data analysis (Fig. 3). Simple and
156 fast cooling, like Paths 1 and 6, or steady and monotonic cooling, like Path 2, produce minimal
157 differences in the data patterns predicted by different kinetics models (Fig. 3). For example,
158 Paths 1 and 6 predict AHe cooling ages with a difference of ~ 1 Myr using the three published
159 kinetics models that account for radiation damage accumulation and annealing effects (Flowers
160 et al. 2009; Gautheron et al., 2009, Willett et al 2017) for crystals with [eU] values ranging from
161 10 ppm to 300 ppm. For the same [eU] apatite crystals, Path 2 predicts cooling ages that differ
162 by between ~ 1 - 5 Myr. In contrast, paths 3, 4, and 5 spend more time at He partial-retention
163 temperatures and therefore produce age-[eU] patterns that are more variable among the
164 kinetics models (Fig. 3).

165 The versions of Path 5 tuned to three radiation damage accumulation and annealing
166 models in the AHe system (Gautheron et al., 2009; Flowers et al., 2009; Willet et al., 2017)
167 provide a particularly instructive result. The peak temperatures required by the Flowers- and
168 Willet-tuned tT paths are within 0.5°C of each other, meaning that they predict a 40 Ma age for a
169 60 µm and 60 ppm [eU] crystal with the effectively identical tT histories. Likewise, at [eU] < 40
170 ppm, the Willet- and Flowers-tuned paths predict very similar ages. However, these models
171 diverge by >20 Myr at [eU] > 90 ppm; in other words, just because the Flowers- and Willet-tuned
172 tT paths are identical does not mean they predict the same ages for all crystal compositions. In



173 contrast, the version of Path 5 tuned to the Gautheron et al. (2009) kinetics model, which has
174 slightly higher peak temperature (Fig. 2), produces an age-[eU] trend that is similar to the Willet-
175 tuned trend at [eU] > 60 ppm, similar to the Flowers- and Willet-tuned models at [eU] = 10 ppm,
176 but different from both the Flowers- and Willet-tuned trends at [eU] = 30 ppm (Fig. 3). Thus,
177 these simple forward models reveal the non-systematic differences among these kinetics
178 models and in what types of thermal histories (i.e., paths 3, 4, and 5) these differences manifest
179 most.

180 In this approach, it is critical to recognize that the largest differences in predicted He
181 ages among kinetics models occurs for the [eU] values that are different from 60 ppm [eU]
182 composition used to tune the paths, i.e., sometimes, but not always, the highest and lowest [eU]
183 crystals in an age-[eU] pattern. This is a result inherent to the particular approach we have
184 taken here: the tuning of the path to a fixed parameter (e.g., [eU] and grain size). The relative
185 difference in cooling ages for each [eU] would be different for paths tuned to a 20 ppm crystal or
186 a 100 ppm crystal. We emphasize that the choice of exactly how to tune a benchmark path
187 depends on the application. Regardless of the details of how a path is tuned, it will always be
188 the case that different kinetics models predict different patterns of data that depend on these
189 parameters, and exploring the sensitivities of each parameter is important to understand in the
190 modeling process.

191 For the ZHe system, the versions of Path 5 tuned to radiation damage accumulation and
192 annealing models of Guenther et al. (2013) and Ginster et al. (2019) have peak temperatures
193 within 0.5°C of each other (Fig. 2), but the predicted age-[eU] distribution is also nearly identical.
194 For these kinetics models, tuned Path 5 thermal histories predict cooling ages within ~ 1 Myr of
195 each other for [eU] values ranging from 100 - 3000 ppm (Fig. 3). This is also true for the other
196 benchmark paths tuned to the Guenther et al. (2013) and Ginster et al., (2019) kinetics
197 models. This suggests that for 100-Myr-long thermal histories, the Guenther and Ginster
198 models will predict similar results. A third kinetics model—which for demonstration purposes



199 simulates only damage accumulation, and not annealing (Guenther, 2021)—has peak
200 temperatures 1.5 - 2°C higher than models that incorporate annealing. This no-annealing model
201 predicts an age-eU trend that only diverges from the others at [eU] > 600 ppm (Fig. 3), at crystal
202 compositions where radiation damage accumulates more rapidly and thus the annealing of this
203 damage is more impactful.

204 Considering the track-length distributions for the AFT system is one way to explore how
205 different AFT kinetics models predict data distributions for crystals with the same chemistry (Fig.
206 3). Although benchmark paths for the Ketcham (1999) and Ketcham et al. (2007) kinetics
207 models predict the same modalities and mean track lengths that vary by a maximum of ~ 0.15
208 µm, the uncertainties of mean track lengths can vary by as much as 0.25 µm. Consequently, the
209 kinetics model of Ketcham et al. (2007) predicts a narrower peak(s) of track lengths for all Paths
210 (Fig. 3). Versions of Path 5 tuned to each kinetics model produce identical mean track lengths,
211 but uncertainty is 0.05 µm lower for track lengths predicted by the Ketcham et al. (2007) kinetics
212 model. Interestingly, the uncertainty in mean track lengths, ~0.25 µm, is greatest for Paths 1
213 and 6 which have simple, fast cooling. This example uses track-length distributions, but
214 modifying other parameters—for example, grain chemistry or its proxy, Dpar—could also be
215 used to explore predictions from different AFT kinetics models.

216

217 **5. A vision for the application of benchmark paths**

218 Here, we demonstrate how a suite of benchmark tT paths can be designed to leverage
219 the temperature sensitivity of a particular low-temperature thermochronometer and then tuned
220 to specific kinetics models. We propose that the six benchmark paths we use in this work can
221 provide a practical tool for the thermochronology community to use in a variety of contexts,
222 including comparing kinetics models and predicting data patterns that arise from variable
223 mineral compositions or geometries. This 'design-then-tune' approach is not meant to identify a
224 single 'best' kinetics model for a particular system but to quantify and visualize how kinetics



225 models predict different tT conditions and data patterns. Having a common framework can also
226 be used in the future to facilitate communicating how new kinetics models differ from existing
227 models. The design and tuning decisions we made here provide a common reference point for
228 interpreting AHe, AFT, and ZHe data, but a single suite of tuned paths cannot capture all
229 complexities of these systems. For example, our proposed benchmark paths span a 100 Myr
230 time frame (Fig. 1)—a time period that may be insufficient for capturing the accumulation of
231 radiation damage and/or annealing that is a hallmark of the AHe and ZHe systems and is
232 captured in those kinetics models. Despite these limitations, we envision that benchmark paths
233 can serve as an entry point to thinking critically about the relationship between the style of a tT
234 history and the kinetic behaviors of chronometric systems that are sensitive to both temperature
235 and time.

236

237 **Competing Interests**

238 All authors are Coordinators for the GChron Special Issue “Technical notes on modelling
239 thermochronologic data” to which this technical note is submitted.

240

241 **Author Contributions**

242 ALSG, KEM, ALA, and MW all contributed to the project design and modeling. ALSG and KEM
243 prepared the manuscript with contributions from all authors.

244

245 **References**

246 Carlson, W. D., Donelick, R. A., and Ketcham, R. A.: Variability of apatite fission-track annealing
247 kinetics : I . Experimental results, *Am. Mineral.*, 84, 1213–1223, 1999.

248 Donelick, R. A., Ketcham, R. A., and Carlson, W. D.: Variability of apatite fission-track annealing
249 kinetics : II . Crystallographic orientation effects, *Am. Mineral.*, 84, 1224–1234, 1999.



- 250 Farley, K. A.: Helium diffusion from apatite: General behavior as illustrated by Durango
251 fluorapatite, *J. Geophys. Res. Solid Earth*, 105, 2903–2914,
252 <https://doi.org/10.1029/1999JB900348>, 2000.
- 253 Flowers, R. M., Ketcham, R. A., Shuster, D. L., and Farley, K. A.: Apatite (U-Th)/He
254 thermochronometry using a radiation damage accumulation and annealing model,
255 *Geochim. Cosmochim. Acta*, 73, 2347–2365, <https://doi.org/10.1016/j.gca.2009.01.015>,
256 2009.
- 257 Gautheron, C., Tassan-Got, L., Barbarand, J., and Pagel, M.: Effect of alpha-damage annealing
258 on apatite (U-Th)/He thermochronology, *Chem. Geol.*, 266, 157–170,
259 <https://doi.org/10.1016/j.chemgeo.2009.06.001>, 2009.
- 260 Ginster, U., Reiners, P. W., Nasdala, L., and Chanmuang N., C.: Annealing kinetics of radiation
261 damage in zircon, *Geochim. Cosmochim. Acta*, 249, 225–246,
262 <https://doi.org/10.1016/j.gca.2019.01.033>, 2019.
- 263 Guenther, W. R.: Implementation of an Alpha Damage Annealing Model for Zircon (U-Th)/He
264 Thermochronology With Comparison to a Zircon Fission Track Annealing Model,
265 *Geochemistry, Geophys. Geosystems*, 22, 1–16,
266 <https://doi.org/10.1029/2019GC008757>, 2021.
- 267 Guenther, W. R., Reiners, P. W., Ketcham, R. A., Nasdala, L., and Giester, G.: Helium
268 diffusion in natural zircon: radiation damage, anisotropy, and the interpretation of zircon
269 (U-TH)/He thermochronology, *Am. J. Sci.*, 313, 145–198,
270 <https://doi.org/10.2475/03.2013.01>, 2013.
- 271 Ketcham, R. A., Donelick, R. A., and Carlson, W. D.: Variability of apatite fission-track annealing
272 kinetics : III . Extrapolation to geological time scales, *Am. Mineral.*, 84, 1235–1255, 1999.



- 273 Ketcham, R. A., Carter, A., Donelick, R. A., Barbarand, J., and Hurford, A. J.: Improved
274 modeling of fission-track annealing in apatite, 92, 799–810,
275 <https://doi.org/10.2138/am.2007.2281>, 2007.
- 276 Murray, K. E., Stevens Goddard, A. L., Abbey, A. L., and Wildman, M.: Thermal history
277 modeling techniques and interpretation strategies: Applications using HeFTy,
278 *Geosphere*, 18, 1622–1642, <https://doi.org/10.1130/GES02500.1>, 2022.
- 279 Reiners, P. W., Spell, T. L., Nicolescu, S., and Zanetti, K. A.: Zircon (U-Th)/He
280 thermochronometry : He diffusion and comparisons with $^{40}\text{Ar} / ^{39}\text{Ar}$ dating, *Geochim.*
281 *Cosmochim. Acta*, 68, 1857–1887, <https://doi.org/10.1016/j.gca.2003.10.021>, 2004.
- 282 Sobel, E. R. and Seward, D.: Influence of etching conditions on apatite fission-track etch pit
283 diameter, *Chem. Geol.*, 271, 59–69, <https://doi.org/10.1016/j.chemgeo.2009.12.012>,
284 2010.
- 285 Willett, C. D., Fox, M., and Shuster, D. L.: A helium-based model for the effects of radiation
286 damage annealing on helium diffusion kinetics in apatite, *Earth Planet. Sci. Lett.*, 477,
287 195–204, <https://doi.org/10.1016/j.epsl.2017.07.047>, 2017.
- 288 Wolf, R. A., Farley, K. A., and Silver, L. T.: Helium diffusion and low-temperature
289 thermochronometry of apatite, *Geochim. Cosmochim. Acta*, 60, 4231–4240,
290 [https://doi.org/10.1016/S0016-7037\(96\)00192-5](https://doi.org/10.1016/S0016-7037(96)00192-5), 1996.
- 291 Wolf, R. A., Farley, K. A., and Kass, D. M.: Modeling of the temperature sensitivity of the apatite
292 (U-Th)/He thermochronometer, *Chem. Geol.*, 148, 105–114,
293 [https://doi.org/10.1016/S0009-2541\(98\)00024-2](https://doi.org/10.1016/S0009-2541(98)00024-2), 1998.